Supplementary Figure S1. EMT phenomena are found in the allografts at early stages of OAD and at later stages under tacrolimus treatment. (a) Experimental design: two tracheas from K5-Cre^{ERT2};Rosa26tdTomato (K5-TOM) mice were transplanted into each C57BL/6 wild-type mouse in the allografts group, or into each CD3ε$^{-/-}$ mouse (CD3εKO) in the "non-rejected grafts" group. All K5-TOM donors were fed with tamoxifen-containing diet to induce tdTomato expression in K5^{+} epithelial lineage. All grafts were harvested at day 7 post-HTT. (b) Cre/Lox efficiency tested on K5-TOM native tracheas by confocal microscopy after 3 weeks of tamoxifen-containing diet. Each data point represent one complete section of trachea. Four different sections were examined for each trachea (n = 2 mice). (c) Representative confocal images of a non-rejected graft compared to an allograft at day 7. The white arrowheads show several tdTomato^{+} cells in the epithelial layer of the allograft that co-stain for αSMA. Bar scale = 200 µm. (d) Confocal analysis quantification showing the fraction of tdTomato^{+} cells that colocalize for αSMA in grafts lumen at day 7 (n = 5-7 grafts). (e) Experimental design: two K5-TOM tracheas were engrafted into each Ubi-GFP mouse. TdTomato expression was induced by tamoxifen-containing diet for 3 weeks. All recipients received either 1mg/kg tacrolimus (T1) or mock IP injections every day until grafts harvesting at day 28 post-HTT. (f) Representative confocal pictures of a tacrolimus-treated allograft at day 28. The white arrowheads indicate some tdTomato^{+} αSMA^{+} cells found in the lumen. Bar scale = 200 µm. (g) Confocal analysis quantification of tdTomato expression among luminal αSMA^{+} cells in mock and T1-treated allografts. Each dot represents one graft (n = 5-8). All data are shown as median values ± interquartile ranges.
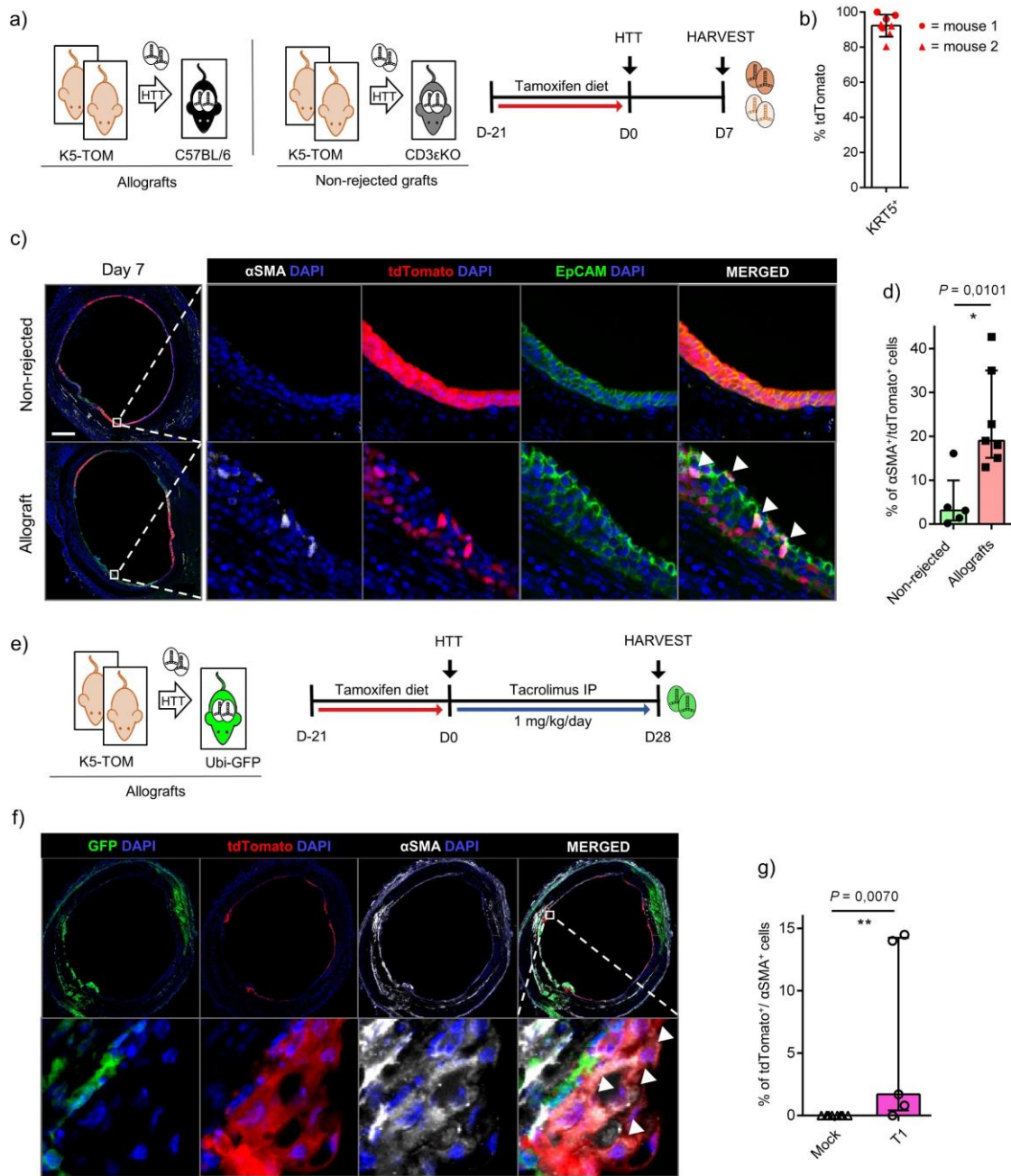
a)

K5-TOM → C57BL/6
Allografts

K5-TOM → CD3εKO
Non-rejected grafts

Tamoxifen diet
D-21 → D0 (HTT) → D7 (HARVEST)

b)

% tdTomato

● = mouse 1
▲ = mouse 2

KRT5⁺

c) Day 7

αSMA DAPI | tdTomato DAPI | EpCAM DAPI | MERGED

Non-rejected

Allograft

d)

% of αSMA⁺/tdTomato⁺ cells

P = 0,0101
*

Non-rejected | Allografts

e)

K5-TOM → Ubi-GFP
Allografts

Tamoxifen diet
D-21 → D0 (HTT) → Tacrolimus IP 1 mg/kg/day → D28 (HARVEST)

f)

GFP DAPI | tdTomato DAPI | αSMA DAPI | MERGED

g)

% of tdTomato⁺/ αSMA⁺ cells

P = 0,0070
**

Mock | T1

Figure S1. EMT phenomena are found in the allografts at early stages of OAD and at later stages under tacrolimus treatment

Supplementary Figure S2. Most myofibroblasts arise from recipient-derived hematopoietic cells. (a) Experimental design: two BALB/c tracheas were implanted subcutaneously into each VAV1-Cre;Rosa26tdTomato (VAV1-TOM) recipient in order to specifically track the recipient-derived hematopoietic lineage (tdTomato$^+$ cells). All allografts and recipients bone marrows were harvested at day 28 post-HTT and analysed respectively by confocal microscopy or flow cytometry. **(b)** Flow cytometry analysis of VAV1-TOM bone marrows (n = 3 mice): quantification of tdTomato expression among CD45$^+$ hematopoietic cells (left) and CD45 expression among all tdTomato$^+$ cells (right). **(c)** Representative confocal images of allografts (BALB/c to VAV1-TOM) at day 28, showing αSMA, tdTomato, CD45 and DAPI co-staining. Bar scale = 200 µm. **(d)** Proportion of αSMA$^+$ myofibroblasts expressing the hematopoietic reporter tdTomato in the lumen fibrosis at day 28, based on confocal analysis (n = 6 allografts).
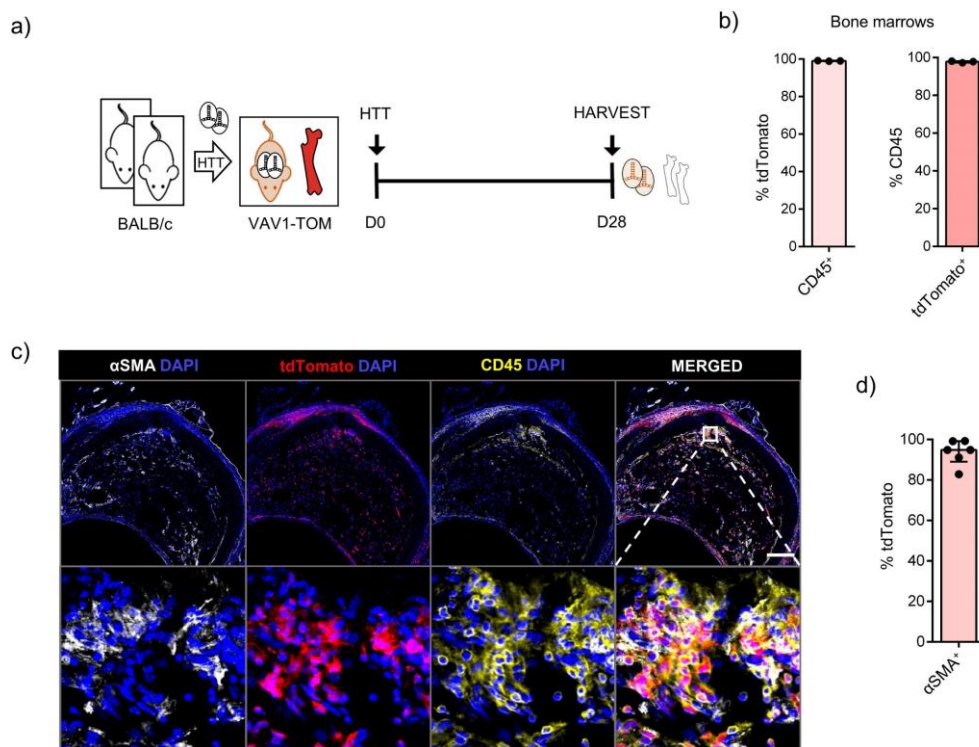

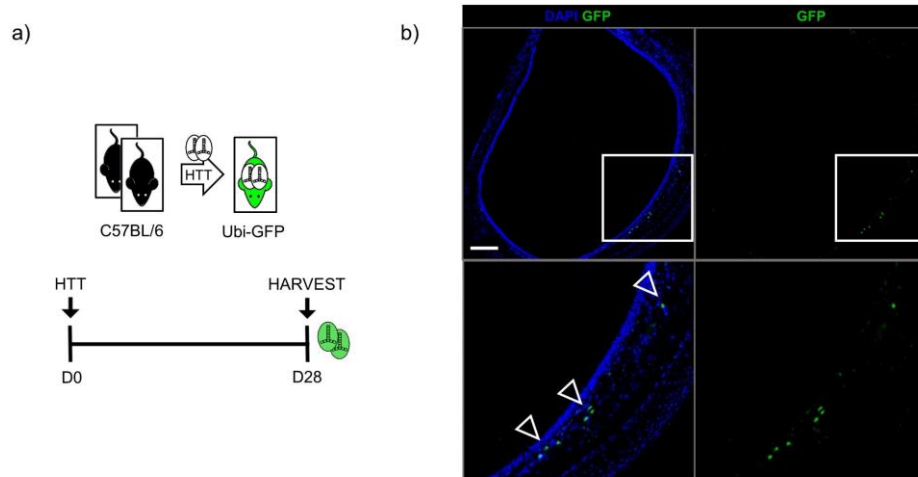Figure S2. Most myofibroblasts arise from recipient-derived hematopoietic cells.
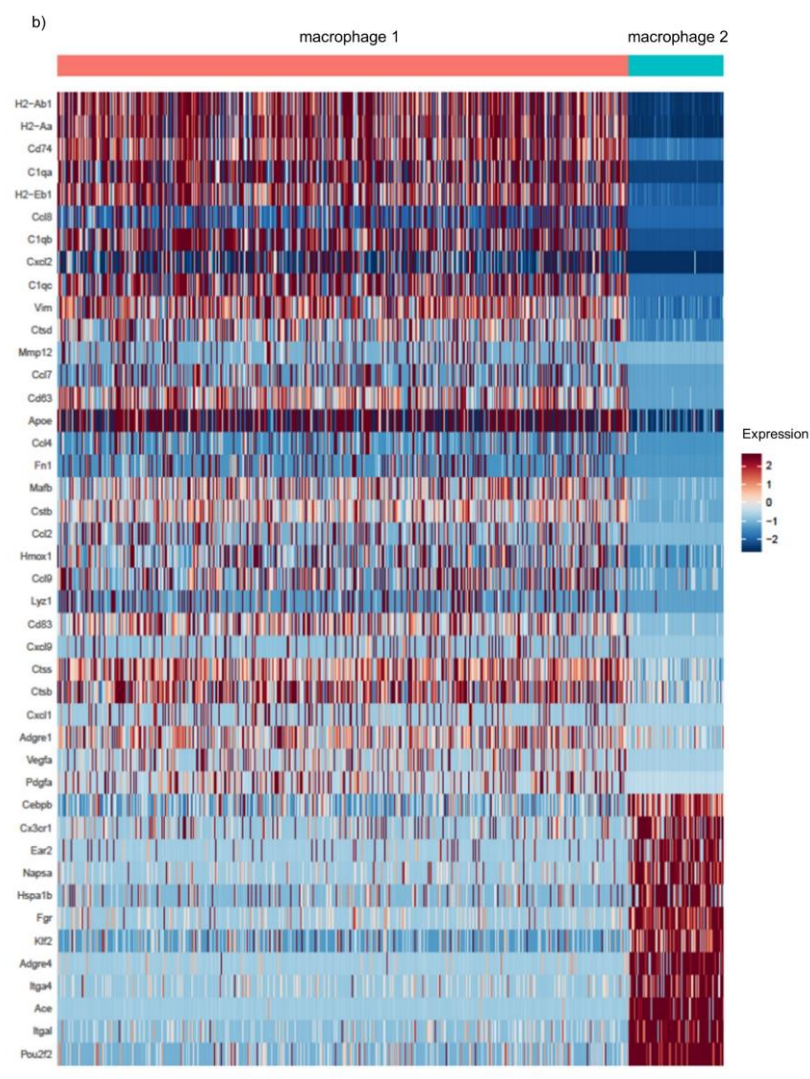
Supplementary Figure S3. Confocal analysis of syngeneic grafts from UbiGFP recipients at day 28 post-HTT. (**a**) Experimental design. (**b**) Confocal images of a syngeneic graft (C57BL/6 trachea into Ubi-GFP recipient) at day 28 after transplantation (representative of 3 independent experiments). The arrows show some GFP$^+$ recipient-derived cells in the submucosa. Bar scale = 200 μm.


Figure S3. Confocal analysis of syngeneic grafts from UbiGFP recipients at day 28 post-HTT.
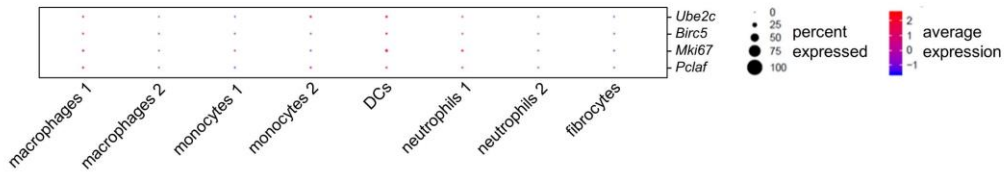
Supplementary Figure S4. ScRNA-seq analysis of tdTomato⁺ cells from LysM-TOM spleen and allografts. (a) Dot plots showing average expression of selected lineage-defining genes across identified clusters [4–6]. (b) Heatmap of genes differentially expressed between the "Macrophages 1" (mainly allograft cells) and "Macrophages 2" (mainly splenocytes) clusters. (c) UMAPs showing the expression of several genes of interest across different clusters. (d) Dot plots representing the expression of specific markers of cell proliferation [7] among each cluster.

a)

b)
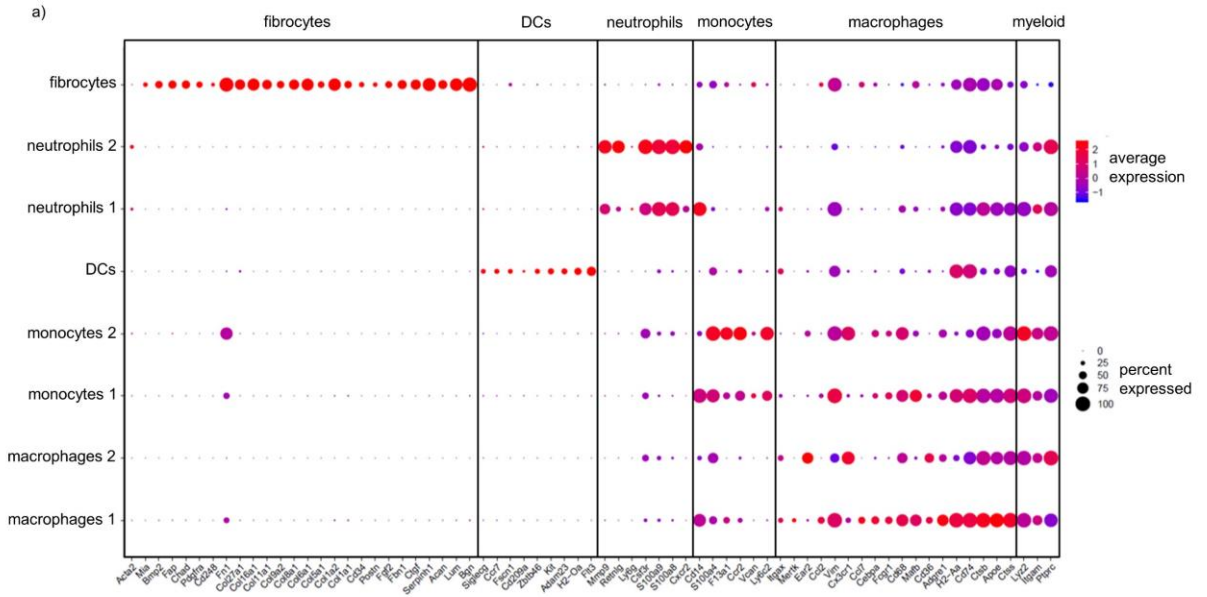
c)
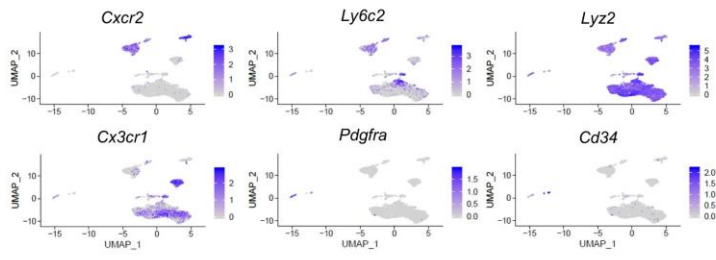
d)

Supplementary Figure S3. ScRNA-seq analysis of tdTomato+ cells from LysM-TOM spleen and allografts.

Supplementary Figure S5. Phenotypic characterization of myeloid-derived αSMA$^+$ cells by flow cytometry. (**a**) Experimental design. The two allografts harvested from the same recipient at day 28 were pooled together before performing flow cytometric analysis. (**b**) Gating strategy for LysM-TOM-derived allografts. (**c**) Proportion of αSMA$^+$ cells expressing or not the myeloid reporter tdTomato among either CD45$^+$ Lin$^-$ or CD45$^-$ Lin$^-$ cells. (**d**) Proportion of Cx3cR1-expressing macrophages (CD45$^+$ LIN$^-$ CD11b$^+$ Ly6G$^-$ Ly6C$^-$ F4.80$^+$), monocytes (CD45$^+$ LIN$^-$ CD11b$^+$ Ly6G$^-$ Ly6C^{hi}) and granulocytes (CD45$^+$ LIN$^-$ CD11b$^+$ Ly6G$^+$) among myeloid-derived (tdTomato$^+$) αSMA$^+$ cells. All data are shown as median values ± interquartile ranges. (**e**) Relative distribution of CD68$^+$ Cx3cR1$^+$ or Cx3cR1$^-$ macrophages (CD45$^+$ LIN$^-$ CD11b$^+$ Ly6G$^-$ Ly6C$^-$), monocytes (CD45$^+$ LIN$^-$ CD11b$^+$ Ly6G$^-$ Ly6C^{hi}), granulocytes (CD45$^+$ LIN$^-$ CD11b$^+$ Ly6G$^+$) and other CD11b$^+$ or CD11b$^-$ populations among myeloid-derived (tdTomato$^+$) αSMA$^+$ cells from allografts at day 28 post-HTT. (c – e) Each dot or bar represents two pooled allografts from the same LysM-TOM recipient (n = 5).
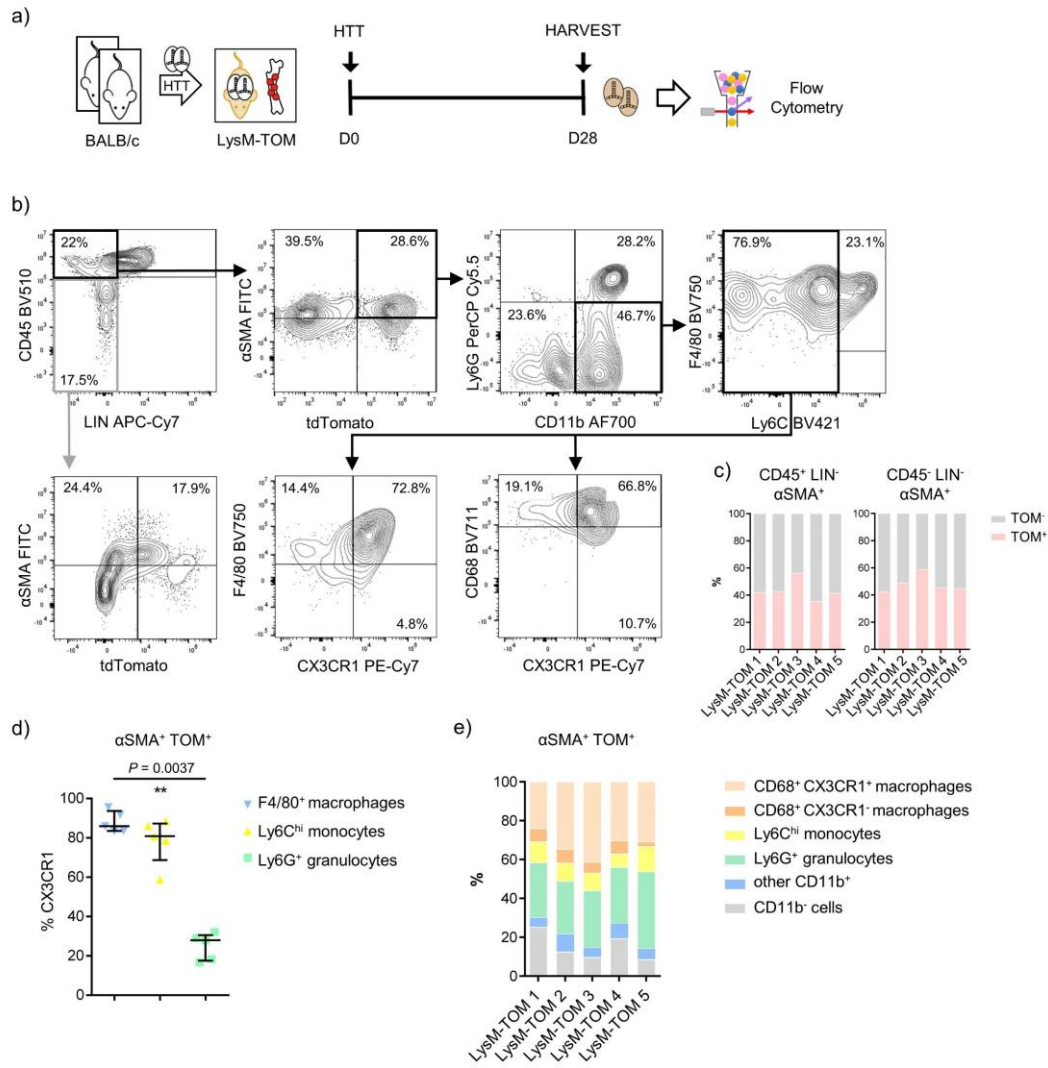
Figure S5. Phenotypic characterization of myeloid-derived αSMA+ cells by flow cytometry.

References

1. Aibar S, González-Blas CB, Moerman T, Huynh-Thu VA, Imrichova H, Hulselmans G, Rambow F, Marine JC, Geurts P, Aerts J, Van Den Oord J, Atak ZK, Wouters J, Aerts S. SCENIC: Single-cell regulatory network inference and clustering. *Nat. Methods* 2017; 14: 1083–1086.

2. Parker MW, Rossi D, Peterson M, Smith K, Sikstroṁ K, White ES, Connett JE, Henke CA, Larsson O, Bitterman PB. Fibrotic extracellular matrix activates a profibrotic positive feedback loop. *J. Clin. Invest.* 2014; 124: 1622–1635.

3. Aran D, Looney AP, Liu L, Wu E, Fong V, Hsu A, Chak S, Naikawadi RP, Wolters PJ, Abate AR, Butte AJ, Bhattacharya M. Reference-based analysis of lung single-cell sequencing reveals a transitional profibrotic macrophage. *Nat. Immunol.* 2019; 20: 163–172

4. Cohen M, Giladi A, Gorki AD, Solodkin DG, Zada M, Hladik A, Miklosi A, Salame TM, Halpern KB, David E, Itzkovitz S, Harkany T, Knapp S, Amit I. Lung Single-Cell Signaling Interaction Map Reveals Basophil Role in Macrophage Imprinting. *Cell* 2018; 175: 1031–1044

5. Scott CL, T'Jonck W, Martens L, Todorov H, Sichien D, Soen B, Bonnardel J, De Prijck S, Vandamme N, Cannoodt R, Saelens W, Vanneste B, Toussaint W, De Bleser P, Takahashi N, Vandenabeele P, Henri S, Pridans C, Hume DA, Lambrecht BN, De Baetselier P, Milling SWF, Van Ginderachter JA, Malissen B, Berx G, Beschin A, Saeys Y, Guilliams M. The Transcription Factor ZEB2 Is Required to Maintain the Tissue-Specific Identities of Macrophages. *Immunity* 2018; 49: 312–325.

6. Schyns J, Bai Q, Ruscitti C, Radermecker C, Schepper S De, Chakarov S, Farnir F, Pirottin D, Ginhoux F, Boeckxstaens G, Bureau F, Marichal T. Non-classical tissue

monocytes and two functionally distinct populations of interstitial macrophages

populate the mouse lung. *Nat. Commun.* 2019; 10: 3964

7.   Morse C, Tabib T, Sembrat J, Buschur KL, Bittar HT, Valenzi E, Jiang Y, Kass DJ,

Gibson K, Chen W, Mora A, Benos P V., Rojas M, Lafyatis R. Proliferating

SPP1/MERTK-expressing macrophages in idiopathic pulmonary fibrosis. *Eur. Respir.*

J. 2019; 54: 1802441